Inorganic Chemistry

Article

pubs.acs.org/IC

Computational Study of the Initial Stage of Diborane Pyrolysis

Baili Sun and Michael L. McKee*

Department of Chemistry and Biochemistry, Auburn University, Auburn, Alabama 36849, United States

Supporting Information

ABSTRACT: The rate constants for the association of two boranes to form diborane are investigated using several methods. The most sophisticated method is the variable reaction coordinate-variational transition state theory (VRC-VTST) which has been developed to handle reactions with no enthalpic barriers. The calculated rate constant of 8.2×10^{-11} cm^3·molecule^{-1}·s^{-1} at 545 K is in good agreement with experiment. The rate constant was also computed using conventional VTST with the G4 composite method. Two variations of the multistep mechanisms for diborane pyrolysis are presented. One is initiated by the step $B_2H_6 \rightleftarrows 2\ BH_3$ while the other begins with $2\ B_2H_6 \rightleftarrows B_3H_9 + BH_3$ as the initial elementary step. Both variations are 3/2 order in diborane and have the same activation energy (G4, 28.65 kcal/mol at 420 K). In contrast, the traditional mechanism involving a B_3H_9 intermediate with C_{3v} symmetry has a higher activation energy (33.37 kcal/mol). The two variations involve a C_2-symmetry penta-coordinate B_3H_9 structure that, while an electronic minimum, is not a stationary point on the free energy path between $B_2H_6 + BH_3 \rightarrow B_3H_7 + H_2$. While the calculated activation barrier is higher than the recently determined experimental barrier, the variation in reported values is large (22.0−29.0 kcal/mol). We discuss possible sources of disagreement between experiment and theory.

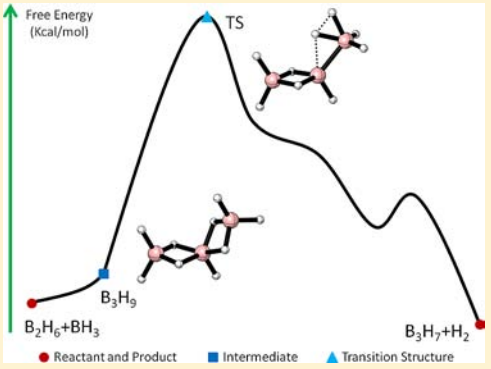

INTRODUCTION

The gas-phase pyrolysis of diborane is considered one of the most complicated processes in the entire field of chemistry.[1] Historically, pyrolysis of diborane has been used to prepare various polyboranes under different conditions.[2] Many experimental studies have been reported on the diborane pyrolysis and decomposition pathways, using such techniques as mass spectrometry,[3−6] chemical vapor deposition,[7−9] isotope exchange,[10−12] and gas chromatography.[13] Unfortunately, controversy surrounding the mechanism has not been resolved, even with the initial stage.[14−16] Generally, the first steps (eq 1 and eq 2a-2c) are as follows:[15−18]

$$B_2H_6 \rightleftarrows 2BH_3 \quad (1)$$

$$B_2H_6 + BH_3 \rightarrow B_3H_7 + H_2 \quad (2a)$$

or

$$B_2H_6 + BH_3 \rightleftarrows B_3H_9 \quad (2b)$$

$$B_3H_9 \rightleftarrows B_3H_7 + H_2 \quad (2c)$$

$$2B_2H_6 \rightleftarrows B_3H_9 + BH_3 \quad (3)$$

It is widely accepted that the symmetric dissociation of diborane initiates the pyrolysis.[19] However, several groups consider that the rate-determining step might be the concerted formation and decomposition of B_3H_9 (eq 2a) or decomposition of B_3H_9 after its formation (eq 2b−2c).[1,17,18] The most recent experiments carried out by Greatrex et al.[17] demonstrated that eq 2a might be the rate-limiting step. An alternative mechanism initiated by eq 3 was also proposed by Long et al.[20a] after an extensive systematic study of boron hydride reactions. This mechanism was also supported by Söderlund et al.[20b] It should be pointed out that eq 3 has been largely ignored in the past decades. We suggest a reappraisal of the contribution of this step.

The 3/2 order dependence of the rate on the diborane concentration in the initial stage has been well established over the temperature range 373 to 550 K with an activation energy in the range of 22.0−29.0 kcal/mol (Table 1).[1,12b,13,14,17,21−26] This strongly implies that a triboron species is involved in the rate-limiting step.[18,21,22] Other important experimental observations include the inhibition by added H_2, which can also alter the product distribution.[14,21,22] Relative rates of pyrolysis of B_2H_6 and B_2D_6 were studied by mass spectrometry, from which a primary isotope effect k_H/k_D of 5.0 was determined,[18b] while a recent experimental reinvestigation yielded a smaller ratio of 2.57.[17] While previous kinetic studies have revealed additional details of this unusually complex reaction, in general, they support the above conclusions.[18,19]

The calculated activation energy can be matched with the observed barrier. For example, if eq 1 is the initial step and eq 2a is the rate-limiting step, the overall reaction activation energy can be expressed as eq 4 where the 1.5 RT term relates activation enthalpy to activation energy for a 3/2 order rate law (rate = $K_1^{1/2}k_{2a}[B_2H_6]^{3/2}$).

Received: January 25, 2013
Published: May 3, 2013

   dx.doi.org/10.1021/ic4001957 | Inorg. Chem. 2013, 52, 5962−5969

Table 1. Reaction Activation Energy (kcal/mol) of the Pyrolysis of Diborane

ΔE_a	temperature (K)	year	ref
	Experimental		
22.0 ± 1.43	398−451	2000	23b
25.6	350−530	1993	26
24.5 ± 0.8	393−453	1989	17
22.1 ± 1.6	323−473	1987	14
10.1 ± 0.3[a]	385−421	1973	25
29.0	343−473	1960	13
27.1 ± 1.0	443−553	1960	23a
27.4	363−383	1951	21
25.5 ± 0.5	373	1951	22
	Calculation		
28.65(G4)	420	2013	this work
28.00(W1BD)	420	2013	this work
27.35[b]	420	2013	this work

[a]The activation barrier was determined with a gas recirculation device. It is not clear why the value is much lower than other results. [b]The enthalpy at 0 K of the $B_2H_6 \rightleftarrows 2\ BH_3$ reaction was taken from quantum Monte Carlo calculations in ref 62 and combined with G4 theory.

$$\Delta E_a = \Delta H^{\ddagger}_{overall} + 1.5RT = 0.5\Delta H_{rx1} + \Delta H^{\ddagger}_{2a} + 1.5RT \quad (4)$$

Two major difficulties are encountered in the experimental studies. First, the intermediates are difficult to identify because of their reactivity.[5,6] Second, because the experiments are generally carried out in a flask, the initial rates are difficult to extract from competing secondary reactions.[3] A noteworthy exception was the study by Fernández et al.[25] where a gas recirculating technique was used to probe the initial rate. Unfortunately, the exceptionally low activation barrier that was obtained for diborane pyrolysis (10.1 kcal/mol) suggests that there was some experimental difficulty.

On the theoretical side, uncertainty exists as to the structure of the intermediates. For example, two isomers of B_3H_9 have been proposed, a cyclic C_{3v} structure and a penta-coordinate C_2 butterfly structure.[27−34] In addition, at least two isomers of B_3H_7 have been proposed, a double-bridged form and a single-bridged form.[27−33] Because of the experimental difficulties of investigating the intermediate steps, high-level theoretical calculations may be the best tool to unravel the reaction mechanism. Over the last 60 years, quantum chemistry calculations have contributed to understanding the structures and reactivity of the boron hydrides.[15,16,29−36] In this work, we have investigated the possible mechanisms of the initial stage of diborane pyrolysis with high-level theory with the hope to shed light on the mechanism.

COMPUTATIONAL METHODS

Frequencies and geometry optimizations for all boron hydrides involved in the reactions (Figure 1) were calculated using the G4 composite method.[37] The accuracy of the B3LYP/6-31G(2df,p) geometries (part of the G4 composite method) was checked by comparing with geometries on the minimum-energy pathway using the CCSD(T)[38−41] method with the 6-311G(d,p) basis set.[42,43] Stationary points in the low-lying pathways were also calculated by using the W1BD composite method.[44] Intrinsic reaction coordinate (IRC)[45] calculations were used to connect the reactant and product through a specific transition structure.

The minimum energy path (MEP) for the barrierless association of two boranes to form diborane has been determined by constrained

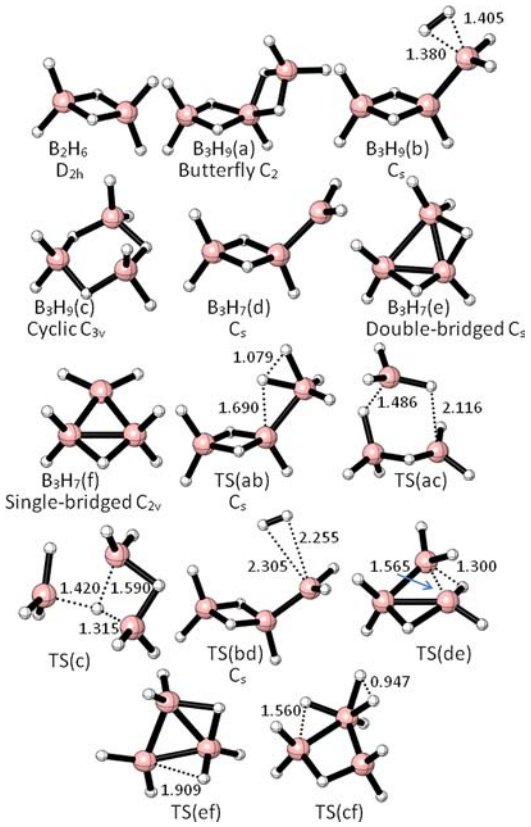

Figure 1. Optimized structures and symmetry designations (except C_1 symmetry) of the reactants, intermediates, and transition structures for the dissociation of B_2H_6 and the reaction of B_2H_6 + BH_3 at the B3LYP/6-31G(2df,p) level. All bond distances are in Angstroms.

optimization fixing the B−B distance to separations of 3.4 to 1.8 Å with a step size of 0.1 Å and optimizing all other variables. Single-point energy calculations at each geometry were made at the G4 level of theory. Vibrational frequencies along the reaction path were calculated after projecting out the reaction coordinate.

Equilibrium constants have been calculated from computed free energies ($K_p = \exp(-\Delta G°/RT)$, where zero-point corrections, heat capacity corrections, and entropies have been included using standard techniques. All electronic structure calculations have been performed using the Gaussian 09 program suite.[46] The direct VRC[47,48]-VTST[49,50] method has been applied to calculate the rate constants of the barrierless association of BH_3 to diborane using the M06/MG3S and M06L/MG3S methods.[51,52] For the reaction $B_3H_9 \rightarrow B_3H_7+H_2$, which has a tight barrier, variational transition state theory with interpolated single-point energies (VTST[49,50]-ISPE,[53] dual-level direct dynamics method) has been used to calculate the rate constants. Geometries and frequencies were generated at the B3LYP/6-31G(2df,p) level of theory, while the reactants, transition struture, and products were redetermined with W1BD theory to improve the reaction energies. Rate constants were further corrected by zero-curvature tunneling (ZCT)[54] and small-curvature tunneling (SCT)[54] for tunneling effects.

Variable reaction coordinate-variational transition state theory (VRC-VTST) was used to investigate the kinetics of association of BH_3, which is very similar to the association of CH_3 radicals. Pivot points were fixed at 0.25 Å along the C_3 axis. A VRC reaction path was constructed by varying the distance between the pivot points in the range of 1.7 Å to 3.4 Å with a 0.1 Å step size. The VRC method avoids the difficulty of computing the interfragment modes where the transition from rotations in the reactants to vibrations in the product is very difficult to treat accurately. The M06/MG3S and M06L/MG3S methods were used because Truhlar and co-workers[55] found these methods to be accurate in the CH_3 association reaction. The rate constants have been calculated using Polyrate.[56] Gaussrate has been

dx.doi.org/10.1021/ic4001957 | Inorg. Chem. 2013, 52, 5962−5969

used as the interface between Gaussian 09 and Polyrate.[57] The natural bond orbital (NBO)[58] analysis was performed using the default NBO package in Gaussian 09.

RESULTS AND DISCUSSION

The potential energy surface (including zero-point energy corrections) involving B_2H_6 + BH_3 was thoroughly explored at the G4 level (Figure 2). Good agreement is found with the

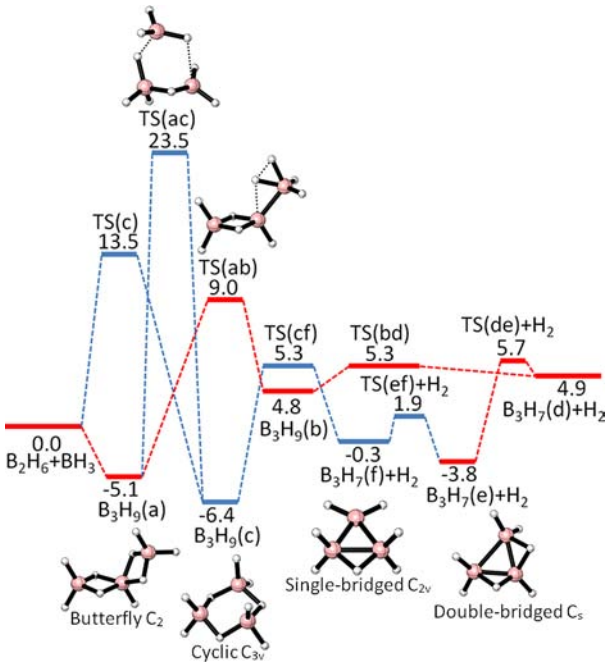

Figure 2. Schematic energy diagram of B_2H_6 + BH_3 at the G4 level of theory. The values are electronic energies plus zero-point corrections in kcal/mol relative to B_2H_6 + BH_3. The red line is the most probable reaction pathway.

transition structure (TS(c)) to form B_3H_9(c) and the transition structure (TS(cf)) to form B_3H_7(f) + H_2 located at the G4 level and those reported by Lipscomb and co-workers[15] at the approximate MP2/6-31G(d) level. In particular, TS(c) features the unusual triple-bridged hydrogen with B−H distances of 1.315, 1.420, and 1.590 Å. The calculated reaction enthalpies at 0 K from B_2H_6 + BH_3 to B_3H_9(c) and to B_3H_7(f) + H_2 agree to within about 3 kcal/mol of those reported by Lipscomb and co-workers[15] at the approximate CCSD(T)/6-31G(d)//MP2/6-31G(d) level. The significant difference between the two studies is the discovery of a new pathway through a penta-coordinate B_3H_9 intermediate with C_2 symmetry (B_3H_9(a)), which is less stable than B_3H_9(c) but is formed from B_2H_6 + BH_3 without an activation barrier. The activation enthalpy (0 K) for elimination of H_2 from B_3H_9(a) is 14.1 kcal/mol, larger than the barrier for loss of H_2 from B_3H_9(c) (11.7 kcal/mol). Through the B_3H_9(a) intermediate, elimination of H_2 has the larger barrier (14.1 kcal/mol), while through the B_3H_9(c) intermediate, formation from B_2H_6 + BH_3 has the larger barrier (13.5 kcal/mol). Duke et al.[27] have described the structure of B_3H_9(a), also known as the butterfly structure, and even predicted that the species could be important in the pyrolysis mechanism of diborane, but they did not report any transition structures.

Both B_3H_9(a) and B_3H_9(c) lose H_2 to form a higher-energy isomer of B_3H_7 (B_3H_7(d) and B_3H_7(f), respectively). However, very small barriers exist for the rearrangement of both to the global minimum B_3H_7(e). From these steps, a mechanism can be postulated for the initial stage of diborane pyrolysis. The elementary step of this mechanism is the dissociation of diborane. Since the reverse reaction is the archetype for all fast boron hydride association reactions and since it has such elegant beauty, it deserves special treatment.

A. Association of BH_3. Although the reaction 2 BH_3 ⇄ B_2H_6 is the inorganic version of the association of two methyl radicals to form ethane, it has not received nearly as much attention. The estimate of the rate constant for BH_3 association at 545 K is 6.6×10^{-11} $cm^3 \cdot molecule^{-1} \cdot s^{-1}$ which is about double the rate for CH_3 association at the same temperature (3.8×10^{-11} $cm^3 \cdot molecule^{-1} \cdot s^{-1}$).[59] This is unusual because the CH_3 association is more than twice as exothermic as the BH_3 association (90.8 kcal/mol versus 36 ± 3 kcal/mol).[6,60,61] It is possible that the motion of the fragments at the bottleneck may be more restricted in the CH_3 association reaction than in the BH_3 association which results in a smaller rate constant. However, the difference in rate constants may be within experimental uncertainly since the experimental rate constant for BH_3 association itself has a large uncertainty.[59]

To confirm the reliability of the level of theory, the symmetric dissociation energies of diborane using various methods have been collected in Table 2. They agree well with

Table 2. Thermochemistry (kcal/mol) for the Dissociation of Diborane to Two BH_3 Fragments

level of theory	ΔE	Δ(E +ZPE)	ΔH(420 K)	ΔG(420 K)
W1BD	44.3	37.9	40.1	25.3
G4	43.6	37.2	39.5	24.6
M06L/MG3S[a]	46.6	42.1	42.1	27.3
CCSD(T)/6-311g(d,p)	42.8	34.1	36.4	21.5
CCSD(T)/6-311++g(3df,2p)	42.5	35.8	38.1	23.2
CCSD(T)/aug-cc-pVTZ	40.8	36.1	38.5	23.5
MP2/aug-cc-pVTZ	44.3	37.6	39.9	24.9
MP2/cc-PVTZ[b]	46.6	39.8	42.1	26.0
diffuse Monte Carlo[c]	43.1	36.6		
exptl[d]		36 ± 3		

[a]Scale factor for vibrational frequencies: 0.978. [b]Scale factor for vibrational frequencies: 0.95. [c]Ref 62. [d]Ref 6.

the experimental range of 36 ± 3 kcal/mol as well as with the most accurate quantum Monte Carlo calculation (36.59 kcal/mol).[6,62] The equilibrium isotope effect for B_2H_6/B_2D_6 computed at the W1BD level at 400 K is K_H/K_D = 2.0, which is the same value reported by Lipscomb and co-workers.[16] See also Figure S-1 in Supporting Information.

Since the association of BH_3 is barrierless, the reaction path was computed by reducing the B−B distance from 3.1 to 1.9 Å in steps of 0.1 Å (Figure 3). At each point along the reaction path, vibrational frequencies were computed by projecting out the transition vector. Free energies at 420 K were computed along the reaction path at the G4 level for B−B separations of 1.9 to 3.1 Å, in this range all of the projected vibrational frequencies are positive. The maximum on the free-energy curve occurs at R(B−B) = 2.9 Å where the free energy is 6.7 kcal/mol higher than at the separated BH_3 fragments. At the B−B distance of 2.9 Å, the enthalpy is 2.6 kcal/mol lower than that of two BH_3 units, consistent with a barrierless reaction. The potential energy surface calculated by DeFrees et al.[63] at

dx.doi.org/10.1021/ic4001957 | Inorg. Chem. 2013, 52, 5962−5969

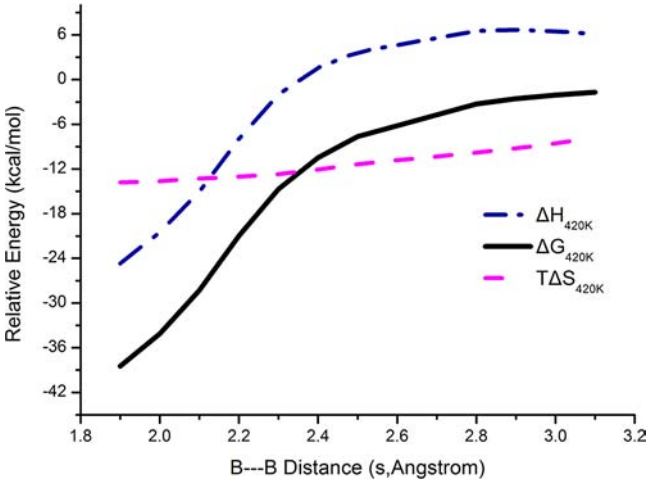

Figure 3. Reaction paths for dissociation of diborane. Quantities calculated at G4 level of theory are enthalpies, free energies, and entropy contributions to free energies. Two BH_3 units at infinite distance are used as reference. The reaction coordinate is the B−B separation.

the MP2/6-31G(d) level of theory is in good agreement with our results.

NBO analysis, an effective tool to study donor−acceptor interactions, has been performed on points along the reaction surface at the MP2/aug-cc-pVTZ level of theory. Comparing second-order perturbative interaction values ($\Delta E^{(2)}$) within NBO theory allows the estimation of stabilization energies which represents the strength of the donor−acceptor interactions.[64] The $\Delta E^{(2)}$ of σ_{B-H} from one BH_3 fragment to the n* orbital of the other BH_3 fragment at the free energy maximum (B−B = 2.9 Å) is 25.3 kcal/mol, while all other interactions are under 1 kcal/mol, indicating that the donor−acceptor interaction of σ_{B-H} with n* is an important interaction in this association. Since the enthalpy at the free energy maximum is not much reduced from that of two boranes, other changes (such as the B−H bond distance) are destabilizing.

The symmetry of the reaction path for dissociation of diborane has been discussed previously.[59,63,65] Angle and bond length changes of diborane along the reaction path have been monitored in Figure 4. From 2.0 Å to 2.6 Å, the B3LYP/6-31G(2df,p) reaction path maintains C_{2h} symmetry. After 2.6 Å, the C_{2h} symmetry is reduced to C_s where the B−H(1)−B and B−H(2)−B angles are unequal. To investigate the origin of symmetry-breaking, NBO analysis was performed along the reaction path at the MP2/aug-cc-pVTZ level of theory (Figure 5). Red/black and green dotted lines represent donor−acceptor stabilization energies along C_s- and C_{2h}-symmetry paths, respectively. The sum of two unequal donor−acceptor interactions in the C_s-symmetry path are larger than the sum of two equal donor−acceptor interactions in the C_{2h}-symmetry path. The overall electronic energy differences are shown in Supporting Information, Table S-1 at the B3LYP/6-31G(2df,p) level of theory. As the boron−boron distance increases from 2.6 to 3.0 Å, the C_s-path becomes more favorable.

The high-pressure limit rate constants of association of BH_3 have been calculated at the M06/MG3S and M06L/MG3S levels of theory (Figure 6) rather than the dissociation rate constants of diborane because there were no direct experimental rate constants for the dissociation process and comparison could be made with the CH_3 radical association

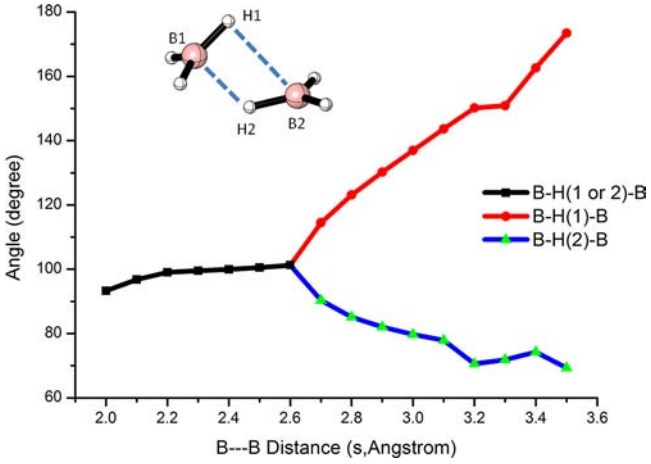

Figure 4. Comparison of two B−H(bridge)−B angle changes along the reaction coordinate. All the geometries are optimized at the B3LYP/6-31G(2df,p) level of theory.

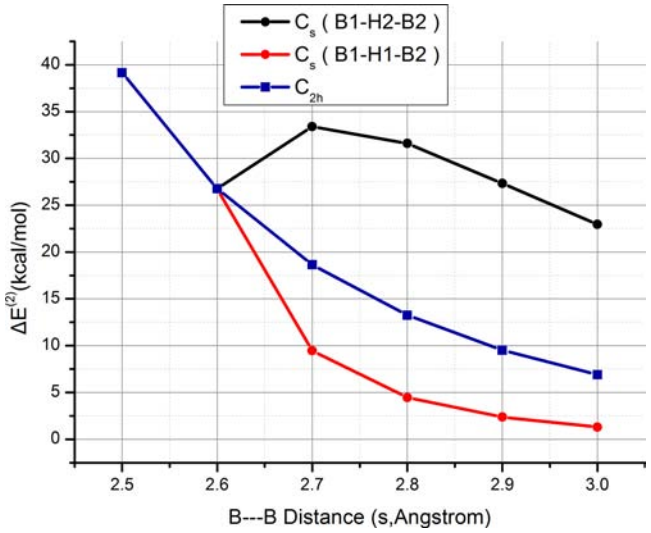

Figure 5. NBO second order donor−acceptor stabilization energies for the dissociation of diborane along the reaction path. "C_s (B1−H2−B2)" and "C_s (B1−H1−B2)" represent the $\sigma_{B-H\rightarrow}$ n* H1−B2 and H2−B1 interactions, respectively, along the C_s reaction path. "C_{2h}" represents the $\sigma_{B-H\rightarrow}$ n* interaction, either H1−B2 or H2−B1.

(for which numerous experimental and computational data are available[55]). The dissociation rate constant of B_2H_6 (needed for the pyrolysis mechanism) can be easily obtained from the forward rate constant and the equilibrium constant. The best experimental determination of the BH_3 association rate constant comes from the association of BH_3 which was produced in the thermal decomposition of BH_3CO.[59] The experimental value corrected to the high pressure limit rate constant at 545 K is $10^{10.6\pm0.4}$ liter·mol^{-1}·s^{-1} or 6.6×10^{-11} cm^3·molecule^{-1}·s^{-1} in units used here. The calculated values evaluated at 550 K are 1.0×10^{-10}, 8.2×10^{-11}, and 1.6×10^{-10} cm^3·molecule^{-1}·s^{-1} at M06L/MG3S with VRC-VTST, M06/MG3S with VRC-VTST, and G4 with VTST, respectively.

B. Pyrolysis of B_2H_6. B1. Unimolecular Step as Initial Step (U path). The present calculations of B_3H_9 and B_3H_7 isomers are in good agreement with previous studies.[15,16,28−36] In the search for the lowest-energy pathway, there has been discussion about whether the reaction proceeds as a two-step

dx.doi.org/10.1021/ic4001957 | Inorg. Chem. 2013, 52, 5962−5969

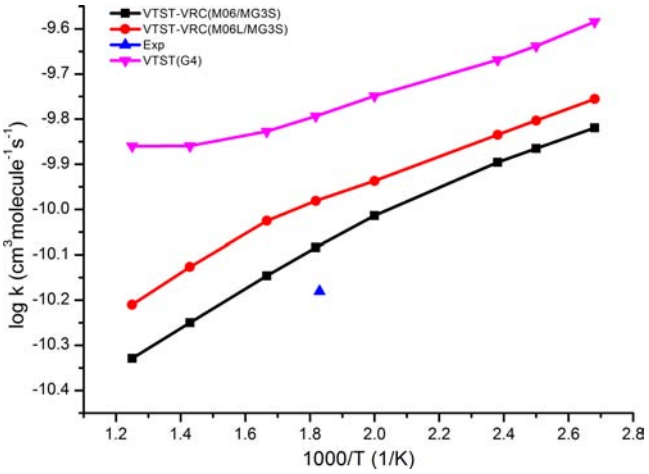

Figure 6. Calculated rate constants for the BH_3 association to B_2H_6. The experimental value is at 545 K.

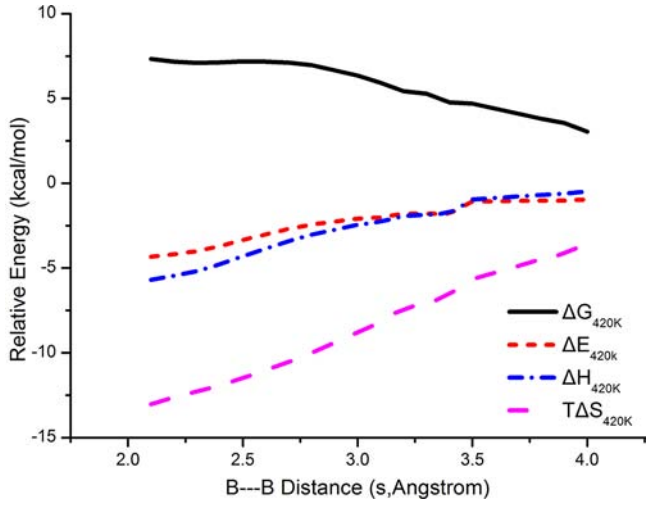

Figure 7. Reaction paths for dissociation of B_3H_9(a) to B_2H_6 + BH_3. Quantities calculated at G4 level of theory are enthalpies, free energies, electronic energies plus zero-point vibrational energies (E_e + ZPE) and entropy contributions to free energies ($T\Delta S$). B_2H_6 plus BH_3 units at infinite distance are used as reference. The reaction coordinate has been projected out.

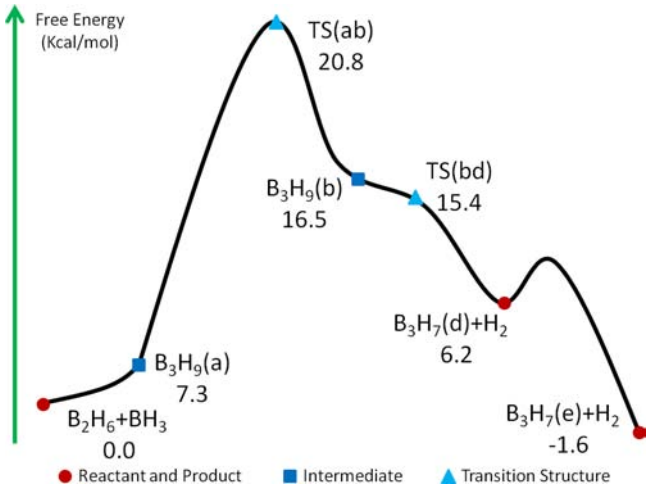

Figure 8. Free energy diagram in kcal/mol of BH_3 reaction with B_2H_6 at the G4 level of theory (420 K).

process with a B_3H_9 intermediate or a single-step process, bypassing the B_3H_9 intermediate. The origin of the debate is that the calculated energy of the B_3H_9 C_{3v}-symmetry structure, when combined with one-half of the B_2H_6 dissociation energy, leads to an activation barrier too large to be consistent with experiment.

The first step of the U path is the dissociation of diborane which is discussed in the section above. The schematic enthalpy (0 K) diagram of the B_2H_6 + BH_3 reactions (Figure 2) is initiated with the barrierless reaction to form B_3H_9(a). The B_3H_9(c) species with C_{3v} symmetry is the most stable isomer of B_3H_9, but it is separated from B_2H_6 + BH_3 by a 13.5 kcal/mol barrier. While the penta-coordinate B_3H_9(a) with four bridging hydrogens and one terminal hydrogen is unknown, the butterfly structure of Al_3H_9 is known in the solid state.[66,67] In addition, a related butterfly structure of B_4H_{10} has been found to play a key role in its reactivity.[68]

From B_3H_9(a), there are two reaction paths; either the butterfly B_3H_9 can isomerize to B_3H_9(c) via a six-membered ring transition structure TS(ac) with an activation barrier of 28.6 kcal/mol followed by hydrogen release via TS(cf) to generate B_3H_7(f) + H_2 or pass over a 14.1 kcal/mol energy barrier via TS(ab). In the transition structure TS(ab), one terminal H atom and one bridging H atom from B_3H_9(a) form an H_2−B_3H_7 complex (B_3H_9(b)) which has a very small barrier for H_2 loss to form B_3H_7(f) + H_2. From the above potential energy surface (PES, including zero-point corrections) of B_2H_6 + BH_3, it is apparent that TS(ab) is involved in the rate-limiting step. Since the addition of BH_3 to B_2H_6 forming B_3H_9(a) is a barrierless reaction, a reaction path was constructed where the B−B distance is decreased in 0.1 Å steps from 3.9 to 2.1 Å (Figure 7). To further explore the rate-limiting step, free energies at 420 K and other thermal properties of the reaction path are shown in Figure 7.

The butterfly B_3H_9(a) is a minimum on the PES (including zero-point corrections). While it is lower in enthalpy (ΔH_{420K}), it is higher in free energy (ΔG_{420K}) relative to B_2H_6 + BH_3. This suggests that B_3H_9(a) is only a minimum at low temperatures while at 420 K, B_3H_9(a) is a point on the reaction path toward B_3H_7(d) + H_2. Thus, the postulated concerted reaction between B_2H_6 + BH_3 → B_3H_7 + H_2 appears to be supported as shown by the free energy surface (420 K) in Figure 8. Except for a small bump when H_2 is lost from B_3H_7(d), the free energy surface at 420 K has the general shape of a concerted process. The free energy barrier is 20.8 kcal/mol, and the overall reaction is spontaneous by 1.6 kcal/mol.

B2. Bimolecular Step as Initial Step (B path). The pyrolysis can also start with a bimolecular reaction between two B_2H_6 molecules. At first glance, entropy consideration would suggest that a bimolecular process could not compete with a unimolecular process except at very high B_2H_6 pressure. However, the products of the bimolecular reaction are B_3H_9 + BH_3 which already form a larger boron hydride. Thus, the first two steps of the "Unimolecular process" are unimolecular + bimolecular while the "Bimolecular process" are bimolecular + unimolecular. In the derivation of the two mechanistic variations, if the first two steps are considered as fast equilibria, the two variations generate the same rate law (see derivations in Supporting Information, Table S-2).

Two bimolecular pathways have been calculated (Figures 9, 10). In the first (Figure 9), the products are B_3H_9(a) + BH_3 (path #1), while in the second (Figure 10), the products are

dx.doi.org/10.1021/ic4001957 | Inorg. Chem. 2013, 52, 5962−5969

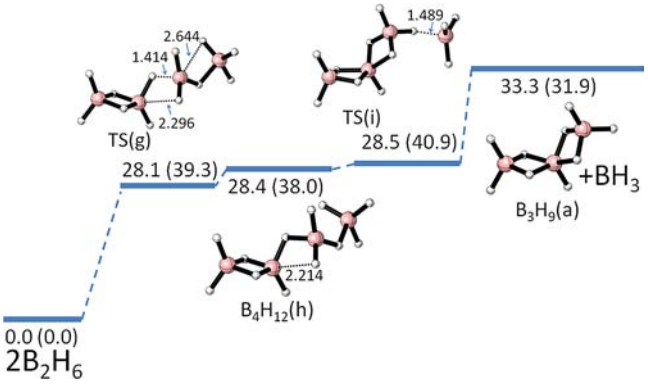

Figure 9. Enthalpy surface for the reaction of B_2H_6 + B_2H_6 → B_3H_9(a,C_2) + BH_3. Enthalpies (kcal/mol) of B_2H_6 + B_2H_6 at 420 K are used as reference. The values in parentheses are free energies, and distances are in Angstroms.

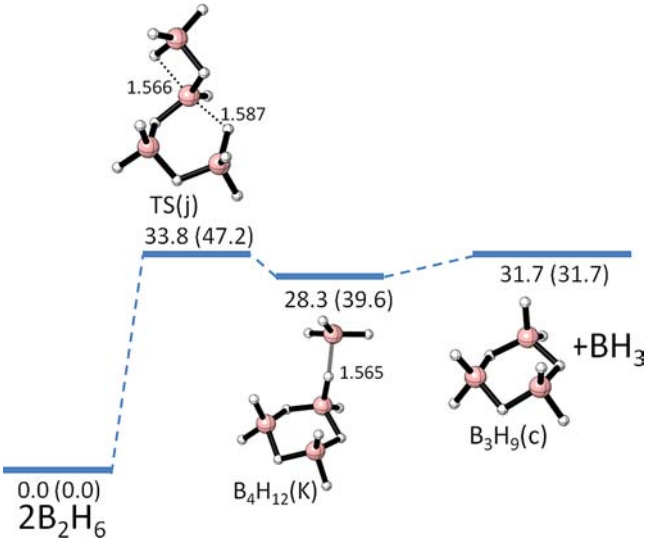

Figure 10. Enthalpy surface for the reaction of B_2H_6 + B_2H_6 → B_3H_9(c,C_{3v}) + BH_3. Enthalpies (kcal/mol) of B_2H_6 + B_2H_6 at 420 K are used as reference. The values in parentheses are free energies and distances are in Angstroms.

B_3H_9(c) + BH_3 (path #2). The first step along the reaction path (path #1) involves the breaking of one hydrogen bridge and forming a new hydrogen bridge in the B_3H_9(a)-BH_3 complex (B_4H_{12}(h)) via transition structure TS(g). The product B_3H_9(a)-BH_3 complex decomposes to B_3H_9(a) and BH_3 via transition structure TS(i). The complex B_4H_{12}(h) and transition structures TS(g) and TS(i) all have very similar enthalpies. One BH_4 structural unit in all three structures (intermediate and transition structures) is nearly static during the reaction.

In the reaction path forming B_3H_9(c) (path #2), the two B_2H_6 molecules unite to form a three-membered ring transition structure (TS(j)). The complex B_4H_{12}(k) loses BH_3 spontaneously by 7.9 kcal/mol at 420 K.

The two pathways (#1 and #2) have free energy barriers (420 K) of 40.9 and 47.2 kcal/mol, respectively, and are endothermic by 33.3 and 33.8 kcal/mol, respectively. Thus, pathway #1 forming B_3H_9(a) is preferred. If the mechanistic derivation assumes fast equilibria for the initial two steps, then the equilibrium constant (not the rate constant) enters the rate law. The following steps of the mechanism involve the reaction of the products (BH_3 and B_3H_9(a)). The BH_3 reacts with B_2H_6 as described above (eq 2b) while B_3H_9(a) decomposes to B_3H_7(d) + H_2 as described above (eq 2c).

B3. General Discussion and Comparison with Experiment. From the above discussion, we propose two possible mechanistic variations. We name them as the Unimolecular (U path) and Bimolecular (B path) paths according to the initial step. In the U path, we propose a reaction mechanism where B_3H_9(a) is treated as an intermediate which forms in a steady state (fast equilibrium).

$$B_2H_6 \rightleftarrows 2BH_3 \quad k_{U1},\ k_{-U1},\ K_{U1} \tag{U1}$$

$$B_2H_6 + BH_3 \rightleftarrows B_3H_7 + H_2 \quad k_{U2},\ k_{-U2},\ K_{U2} \tag{U2}$$

$$B_2H_6 + B_3H_7 \rightarrow B_4H_{10} + BH_3 \quad k_{U3} \tag{U3}$$

$$\text{Rate expression} = -\frac{d(B_2H_6)}{dt} = 2k_{U3}[B_2H_6]\frac{K_{U1}^{1/2}k_{U2}[B_2H_6]^{3/2}}{k_{-U2}[H_2] + k_{U3}[B_2H_6]}$$

$$\Delta E_a = \Delta H^{\ddagger}_{overall} + 1.5RT = 0.5\Delta H_{U1} + \Delta H^{\ddagger}_{U2} + 1.5RT \quad \text{when} \quad k_{U3}[B_2H_6] >> k_{-U2}[H_2]$$

In the initial stage, $k_{U3}[B_2H_6] \gg k_{-U2}[H_2]$, the right-hand side simplifies to $2K_{U1}{}^{1/2}k_{U2}[B_2H_6]^{3/2}$. The calculated activation energies (420 K) at the G4 and W1BD levels of theory are 28.65 and 28.00 kcal/mol, respectively. When the partial pressure of H_2 becomes significant, the rate of the pyrolysis is predicted to decrease which is consistent with experimental observations.[14] The overall pyrolysis rate constants ($k_{overall}$ = $2K_{U1}{}^{1/2}k_{U2}$) calculated by various methods (Table 3) are

Table 3. Rate Constants ($cm^{3/2}$·$molecule^{-1/2}$·s^{-1}) of the Pyrolysis of B_2H_6 at 420 K[a,b]

	k_{U2}[d]				
K_{U1}[c]	CVT	TST/ZCT	CVT/ZCT	TST/SCT	CVT/SCT
W1BD	2.99×10^{-14}	2.23×10^{-14}	3.43×10^{-14}	2.38×10^{-14}	3.67×10^{-14}
G4	4.41×10^{-14}	3.30×10^{-14}	5.06×10^{-14}	3.53×10^{-14}	5.43×10^{-14}
M06L/MG3S	8.73×10^{-15}	6.49×10^{-16}	1.00×10^{-14}	6.98×10^{-16}	1.07×10^{-14}
MP2/cc-pVTZ	1.95×10^{-14}	1.45×10^{-14}	2.24×10^{-14}	1.56×10^{-14}	2.40×10^{-14}
exptl[e]			$(1.86 \pm 0.36) \times 10^{-11}$		

[a] $k_{(overall)} = 2K_{U1}{}^{1/2}k_{U2}$. [b] The rate constant, k_{U2}, is computed with the VTST-ISPE method. The geometries at the reaction path were calculated at the B3LYP/6-31G(2df,p) level. The higher-level electronic structure calculations at the W1BD level were used to correct the energies along the reaction path. [c] W1BD, G4, M06L/MG3S, and MP2/cc-pVTZ are the levels of theory used to calculate K_{U1}. [d] CVT, TST/ZCT, CVT/ZCT, TST/SCT, and CVT/SCT are the methods used to correct the rate constants in eq U2 for tunneling effects (see Polyrate manual). [e] Ref 16.

dx.doi.org/10.1021/ic4001957 | Inorg. Chem. 2013, 52, 5962−5969

smaller than experiment by 3 orders of magnitude. Deuterium isotope effects of k_H/k_D have also been explored in Table 4.

Table 4. Ratio of Rate Constants (k_H/k_D) for the Pyrolysis of B_2H_6/B_2D_6 at 420 K[a–d]

	CVT	TST/ZCT	CVT/ZCT	TST/SCT	CVT/SCT
W1BD	2.25	1.54	1.83	1.60	3.75
G4	2.22	1.53	1.82	1.59	3.70
M06L/MG3S	2.34	1.61	1.93	1.68	3.90
MP2/cc-pVTZ	1.94	1.34	1.60	1.39	3.26
exptl[e]			1.92–3.22		
exptl[f]			5		

[a] $k_{(overall)} = 2K_{U1}^{1/2}k_{U2}$. [b] The rate constant, k_{U2}, is computed with the VTST-ISPE method. The geometries at the reaction path were calculated at B3LYP/6-31G(2df,p) level. The higher-level electronic structure calculations at W1BD level were used to correct the energies along the reaction path. [c] W1BD, G4, M06L/MG3S, and MP2/cc-pVTZ are the levels of theory used to calculate K_{U1}. [d] CVT, TST/ZCT, CVT/ZCT, TST/SCT, and CVT/SCT are the methods used to correct the rate constants in eq U2 for tunneling effects (see Polyrate manual). [e] Ref 17. [f] Ref 18b.

Our results are in the range of a recent experiment at 420 K, but disagree with Enrione et al.[18b] at 361 K. Our calculated ratios are in satisfactory agreement with recent experimental results if experimental uncertainties are considered.[17]

In the B path the steady-state approximation was employed along with the sum of reaction B1 and -B2 (gives $B_2H_6 \rightleftarrows 2\,BH_3$) to derive a mechanistic rate law. The B path was proposed originally by Long et al.[20a] who made a careful analysis of previous experiment work.

$$2B_2H_6 \rightleftarrows BH_3 + B_3H_9(a) \quad k_{B1},\ k_{-B1},\ K_{B1} \tag{B1}$$

$$BH_3 + B_2H_6 \rightleftarrows B_3H_9(a) \quad k_{B2},\ k_{-B2},\ K_{B2} \tag{B2}$$

$$B_3H_9(a) \rightarrow B_3H_7 + H_2 \quad k_{B3} \tag{B3}$$

$$B_2H_6 + B_3H_7 \rightarrow B_4H_{10} + BH_3 \quad k_{U3} \tag{U3}$$

$$\text{Rate expression} = -\frac{d(B_2H_6)}{dt} = 2K_{B1}^{1/2}K_{B2}^{1/2}k_{B3}[B_2H_6]^{3/2}$$

$$\Delta E_a = \Delta H^{\ddagger}_{overall} + 1.5RT = 0.5(\Delta H_{B1} + \Delta H_{B2}) + \Delta H^{\ddagger}_{B3} + 1.5RT$$

The calculated reaction activation energy is 28.65 kcal/mol, the same as the U path at 420 K at the same level of theory. As can be seen in Table 1, the theoretical values are within the range of the experimentally determined values for the pyrolysis of diborane.

The rate of consumption of diborane can be accelerated through diborane scavenging reactions such as reaction U3. As the reaction proceeds, many additional reactive intermediates are formed which can also react with B_2H_6. Thus, additional reactions will deplete B_2H_6 in competition with the initial reactions and may have the overall effect of reducing the effective activation barrier and increasing the consumption rate of diborane. These additional scavenging reactions are probably the reason that the calculated pyrolysis activation barrier is larger than recently determined experimental barriers and why the calculated rate constant is 3 orders of magnitude smaller than the observed rate constant.

CONCLUSION

The gas-phase kinetics of the initial stage of diborane pyrolysis has been probed at different levels of theory with variational transition state theory (VTST). The B_3H_9 isomer with C_{3v} symmetry does not play a role in the pyrolysis mechanism. Instead, a novel B_3H_9 butterfly structure with C_2 symmetry is on the free energy surface between $B_2H_6 + BH_3$ and $B_3H_7 + H_2$. The overall activation barrier is 28.65 kcal/mol at the G4 level. Two reaction variations have been proposed to elucidate the pyrolysis of diborane (U and B paths) which differ by the initial reaction step (unimolecular or bimolecular). Both variations reduce to the same rate law if the initial steps are assumed to be in fast equilibrium. Our long-term goal is to unravel the entire process to the formation of $B_{10}H_{14}$.

ASSOCIATED CONTENT

Supporting Information

A plot of the ratio of equilibrium constants of dissociation of B_2H_6 and B_2D_6 is given in Figure S-1. The overall electronic energy differences between C_s- and C_{2h}-symmetry paths is given in Table S-1. The derivations of the rate law expressions for the U Path and B Path are given in Table S-2. A table including enthalpy (0 K), enthalpy (420 K) and free energy (420 K) of all the stationary points at the G4 level of theory is presented in Table S-3. The Cartesian coordinates of geometries optimized at the B3LYP/6-31G(2df,p) level of theory are given in Table S-4. This material is available free of charge via the Internet at http://pubs.acs.org.

AUTHOR INFORMATION

Corresponding Author

*E-mail: mckee@chem.auburn.edu.

Notes

The authors declare no competing financial interest.

ACKNOWLEDGMENTS

We thank the Alabama Supercomputer Center for providing the computer time. We thank Professor Donald G. Truhlar for providing the Polyrate program.

REFERENCES

(1) Greenwood, N. N. *Chem. Soc. Rev.* **1992**, *21*, 49.
(2) Stock, A. *The Hydrides of Boron and Silicon*; Cornell University Press: New York, 1933.
(3) Baylis, A. B.; Pressley, G. A.; Stafford, F. E. *J. Am. Chem. Soc.* **1966**, *88*, 2428.
(4) Stafford, F. E.; Pressley, G. A.; Baylis, A. B. In *Mass Spectrometry in Inorganic Chemistry*; American Chemical Society: Washington, DC, 1968; Vol. *72*, p 137.
(5) Fehlner, T. P.; Fridmann, S. A. *Inorg. Chem.* **1970**, *9*, 2288.
(6) Fehlner, T. P.; Mappes, G. W. *J. Chem. Phys.* **1969**, *73*, 873.
(7) Rayar, M.; Supiot, P.; Veis, P.; Gicquel, A. *J. Appl. Phys.* **2008**, *104*, 033304.
(8) Mehta, B.; Tao, M. *J. Electrochem. Soc.* **2005**, *152*, G309.
(9) Mohammadi, V.; de Boer, W. B.; Nanver, L. K. *Appl. Phys. Lett.* **2012**, *101*, 111906.
(10) Rigden, J. S.; Koski, W. S. *J. Am. Chem. Soc.* **1961**, *83*, 552.
(11) Maybury, P. C.; Koski, W. S. *J. Chem. Phys.* **1953**, *21*, 742.
(12) (a) Todd, J. E.; Koski, W. S. *J. Am. Chem. Soc.* **1959**, *81*, 2319. (b) Koski, W. S. In *Borax to Boranes*, American Chemical Society: Washington, DC, 1961; Vol *32*, pp 78–87.

(13) Borer, K.; Littlewood, A. B.; Phillips, C. S. G. *Inorg. Nucl. Chem.* **1960**, *15*, 316.
(14) Greenwood, N. N.; Greatrex, R. *Pure Appl. Chem.* **1987**, *59*, 857.
(15) Stanton, J. F.; Lipscomb, W. N.; Bartlett, R. J. *J. Am. Chem. Soc.* **1989**, *111*, 5165.
(16) Lipscomb, W. N.; Stanton, J. F.; Connick, W. B.; Magers, D. H. *Pure Appl. Chem.* **1991**, *63*, 335.
(17) Greatrex, R.; Greenwood, N. N.; Lucas, S. M. *J. Am. Chem. Soc.* **1989**, *111*, 8721.
(18) (a) A brief summary of early kinetic studies of diborane pyrolysis is provided in the following: *Production of the Boranes and Related Research*; Holzmann, R. T., Ed.; Academic Press: New York, 1967; pp 90−115. (b) Enrione, R. E.; Schaeffer, R. J. *Inorg. Nucl. Chem.* **1961**, *15*, 103.
(19) Fehlner, T. P. In *Boron Hydride Chemistry*; Muetterties, E. L., Ed.; Academic Press: New York, 1975, and references cited therein.
(20) (a) Long, L. H. *J. Inorg. Nucl. Chem.* **1970**, *32*, 1097. (b) Söderlund, M.; Mäki-Arvela, P.; Eränen, K.; Salmi, T.; Rahkola, R.; Murzin, D. Y. *Catal. Lett.* **2005**, *105*, 191.
(21) Clarke, R. P.; Pease, R. N. *J. Am. Chem. Soc.* **1951**, *73*, 2132.
(22) Bragg, J. K.; Mccarty, L. V.; Norton, F. J. *J. Am. Chem. Soc.* **1951**, *73*, 2134.
(23) (a) Owen, A. J. *J. Appl. Chem.* **1960**, *10*, 483. (b) Attwood, M. D.; Greatrex, R.; Greenwood, N. N.; Potter, C. D. *J. Organomet. Chem.* **2000**, *614*, 144.
(24) McCarty, L. V.; Giorgio, P. A. D. *J. Am. Chem. Soc.* **1951**, *73*, 3138.
(25) Fernández, H.; Grotewold, J.; Previtali, C. M. *J. Chem. Soc., Dalton Trans.* **1973**, 2090.
(26) Colket, M. B.; Montgomery, J. A. J. *Presentation to the Joint Technical Meeting of the Eastern States and Central States of the Combustion Institute*, New Orleans, LA, 1993.
(27) Duke, B. J.; Gauld, J. W.; Schaefer, H. F. *J. Am. Chem. Soc.* **1995**, *117*, 7753.
(28) Stanton, J. F.; Lipscomb, W. N.; Bartlett, R. J.; Mckee, M. L. *Inorg. Chem.* **1989**, *28*, 109.
(29) Stanton, J. F.; Bartlett, R. J.; Lipscomb, W. N. *Chem. Phys. Lett.* **1987**, *138*, 525.
(30) Olson, J. K.; Boldyrev, A. I. *Inorg. Chem.* **2009**, *48*, 10060.
(31) Mckee, M. L. *J. Phys. Chem.* **1990**, *94*, 435.
(32) McKee, M. L. *J. Am. Chem. Soc.* **1990**, *112*, 6753.
(33) Tian, S. X. *J. Phys. Chem. A* **2005**, *109*, 5471.
(34) Duke, B. J.; Liang, C. X.; Schaefer, H. F. *J. Am. Chem. Soc.* **1991**, *113*, 2884.
(35) Olah, G. A.; Surya Prakash, G. K.; Rasul, G. *Proc. Natl. Acad. Sci. U.S.A.* **2012**, *109*, 6825.
(36) Yao, Y.; Hoffmann, R. *J. Am. Chem. Soc.* **2011**, *133*, 21002.
(37) Curtiss, L. A.; Redfern, P. C.; Raghavachari, K. *J. Chem. Phys.* **2007**, *126*, 084108.
(38) Purvis, G. D., III; Bartlett, R. J. *J. Chem. Phys.* **1982**, *76*, 1910.
(39) Raghavachari, K.; Trucks, G. W.; Pople, J. A.; Head-Gordon, M. *Chem. Phys. Lett.* **1989**, *157*, 479.
(40) Watts, J. D.; Gauss, J.; Bartlett, R. J. *J. Chem. Phys.* **1993**, *98*, 8718.
(41) Bartlett, R. J.; Musial, M. *Rev. Mod. Phys.* **2007**, *79*, 291.
(42) Ditchfield, R.; Hehre, W. J.; Pople, J. A. *J. Chem. Phys.* **1972**, *56*, 2257.
(43) Krishnan, R.; Binkley, J. S.; Seeger, R.; Pople, J. A. *J. Chem. Phys.* **1980**, *72*, 650.
(44) Barnes, E. C.; Petersson, G. A.; Montgomery, J. A.; Frisch, M. J.; Martin, J. M. L. *J. Chem. Theory Comput.* **2009**, *5*, 2687.
(45) Fukui, K. *Acc. Chem. Res.* **1981**, *14*, 363.
(46) Frisch, M. J.; Trucks, G. W.; Schlegel, H. B.; Scuseria, G. E.; Robb, M. A.; Cheeseman, J. R.; Montgomery, Jr., J. A.; Vreven, T.; Kudin, K. N.; Burant, J. C.; Millam, J. M.; Iyengar, S. S.; Tomasi, J.; Barone, V.; Mennucci, B.; Cossi, M.; Scalmani, G.; Rega, N.; Petersson, G. A.; Nakatsuji, H.; Hada, M.; Ehara, M.; Toyota, K.; Fukuda, R.; Hasegawa, J.; Ishida, M.; Nakajima, T.; Honda, Y.; Kitao, O.; Nakai, H.; Klene, M.; Li, X.; Knox, J. E.; Hratchian, H. P.; Cross, J. B.; Bakken, V.; Adamo, C.; Jaramillo, J.; Gomperts, R.; Stratmann, R. E.; Yazyev, O.; Austin, A. J.; Cammi, R.; Pomelli, C.; Ochterski, J. W.; Ayala, P. Y.; Morokuma, K.; Voth, G. A.; Salvador, P.; Dannenberg, J. J.,; Zakrzewski, V. G.; Dapprich, S.; Daniels, A. D.; Strain, M. C.; Farkas, O.; Malick, D. K.; Rabuck, A. D.; Raghavachari, K.; Foresman, J. B.; Ortiz, J. V.; Cui, Q.; Baboul, A. G.; Clifford, S.; Cioslowski, J.; Stefanov, B. B.; Liu, G.; Liashenko, A.; Piskorz, P.; Komaromi, I.; Martin, R. L.; Fox, D. J.; Keith, T.; Al-Laham, M. A.; Peng, C. Y.; Nanayakkara, A.; Challacombe, M.; Gill, P. M. W.; Johnson, B.; Chen, W.; Wong, M. W.; Gonzalez, C.; Pople, J. A. *Gaussian09*; Gaussian Inc.: Pittsburgh, PA, 2009.
(47) Klippenstein, S. J. *J. Chem. Phys.* **1991**, *94*, 6469.
(48) Klippenstein, S. J. *J. Chem. Phys.* **1992**, *96*, 367.
(49) Truhlar, D. G.; Isaacson, A. D.; Garrett, B. C. In *Theory of Chemical Reaction Dynamics*; Baer, M., Ed.; CRC Press: Boca Raton, FL, 1985; Vol 4, pp 65−137.
(50) Truhlar, D. G.; Garrett, B. C. *Acc. Chem. Res.* **1980**, *13*, 440.
(51) Zhao, Y.; Truhlar, D. G. *Theor. Chem. Acc.* **2008**, *120*, 215.
(52) Zhao, Y.; Truhlar, D. G. *Acc. Chem. Res.* **2008**, *41*, 157.
(53) Chuang, Y.-Y.; Corchado, J. C.; Truhlar, D. G. *J. Phys. Chem. A* **1999**, *103*, 1140.
(54) Chuang, Y.-Y.; Truhlar, D. G. *J. Phys. Chem. A* **1997**, *101*, 3808.
(55) Zheng, J.; Zhang, S. X.; Truhlar, D. G. *J. Phys. Chem. A* **2008**, *112*, 11509.
(56) Zheng, J., et al.. *Polyrate 2010-A*; University of Minnesota: Minneapolis, MN, 2010.
(57) Zheng, J.; Zhang, S.; Corchado, J. C.; Chuang, Y.-Y.; Coitiño, E. L.; Ellingson, B. A.; Truhlar, D. G. *Gaussrate 2009-A*; University of Minnesota: Minneapolis, MN, 2010.
(58) Glendening, E. D.; Reed, A. E.; Carpenter, J. E.; Weinhold, F. *NBO Version 3.1*.
(59) Mappes, G. W.; Fridmann, S. A.; Fehlner, T. P. *J. Phys. Chem.* **1970**, *74*, 3307.
(60) Baulch, D. L.; Cobos, C. J.; Cox, R. A.; Esser, C.; Frank, P.; Just, T.; Kerr, J. A.; Pilling, M. J.; Troe, J.; Walker, R. W.; Warnatz, J. *J. Phys. Chem. Ref. Data.* **1992**, *21*, 411.
(61) Baulch, D. L.; Cobos, C. J.; Cox, R. A.; Frank, P.; Hayman, G.; Just, T.; Kerr, J. A.; Murrells, T.; Pilling, M. J.; Troe, J.; Walker, R. W.; Warnatz, J. *J. Phys. Chem. Ref. Data.* **1994**, *23*, 847.
(62) Fracchia, F.; Bressanini, D.; Morosi, G. *J. Chem. Phys.* **2011**, *135*, 094503.
(63) Defrees, D. J.; Raghavachari, K.; Schlegel, H. B.; Pople, J. A.; Schleyer, P. v. R. *J. Phys. Chem.* **1987**, *91*, 1857.
(64) Reed, A. E.; Curtiss, L. A.; Weinhold, F. *Chem. Rev.* **1988**, *88*, 899.
(65) Dixon, D. A.; Pepperberg, I. M.; Lipscomb, W. N. *J. Am. Chem. Soc.* **1974**, *96*, 1325.
(66) Duke, B. J.; Gauld, J. W.; Schaefer, H. F. *Chem. Phys. Lett.* **1991**, *230*, 306.
(67) Nold, C. P.; Head, J. D. *J. Phys. Chem. A* **2012**, *116*, 4348.
(68) (a) McKee, M. L. *Inorg. Chem.* **1986**, *25*, 3545−3547. (b) Ramakrishna, V.; Duke, B. J. *Inorg. Chem.* **2004**, *43*, 8176. (c) Sayin, H.; McKee, M. L. *Inorg. Chem.* **2007**, *46*, 2883. (d) Bühl, M.; McKee, M. L. *Inorg. Chem.* **1998**, *37*, 4953.